Macromolecules

Article

pubs.acs.org/Macromolecules

Effect of Solvent Selectivity on Chain Exchange Kinetics in Block Copolymer Micelles

En Wang,[†] Jiahao Zhu,[†] Dan Zhao,[‡] Shuyi Xie,[‡] Frank S. Bates,[†] and Timothy P. Lodge*,[†,‡]

[†]Department of Chemical Engineering and Materials Science and [‡]Department of Chemistry, University of Minnesota, Minneapolis, Minnesota 55455, United States

Supporting Information

ABSTRACT: The effect of solvent selectivity on the chain exchange kinetics for two polystyrene-*b*-poly(ethylene-*alt*-propylene) block copolymer micelles (SEP 26−70 and SEP 42−64, where the number denotes the molecular weight of each block in kg/mol) is investigated in pure squalane and in binary mixed solvents of squalane and 1-phenyldodecane, using time-resolved small-angle neutron scattering (TR-SANS). The exchange rate accelerates by 5 orders of magnitude for both micelles when adding only 25 vol % 1-phenyldodecane to squalane, compared to micelles in pure squalane. This acceleration is attributed to two factors: faster relaxation dynamics of the core blocks as more solvent penetrates into the core, serving as a plasticizer, combined with a reduced energy barrier for chain expulsion due to the lower Flory−Huggins interaction parameter χ between the core block and the solvent. By fitting the TR-SANS data to an established theoretical model, the enthalpic penalty of chain expulsion is determined for SEP micelles in mixed solvents. These results are quantified by a χ-dependent function derived from Flory−Huggins theory, where χ values between the polystyrene (PS) core block and binary mixed solvents are estimated by a combination of static light scattering and cloud point measurements with PS homopolymers. This work quantifies the role of χ in chain exchange kinetics of block copolymer micelles.

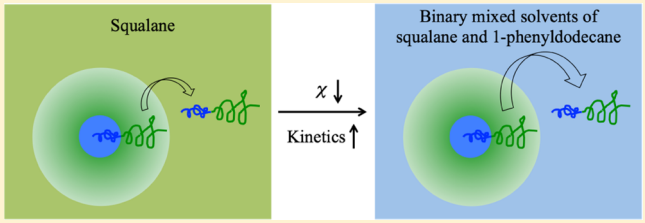

INTRODUCTION

Self-assembled block copolymer (BCP) micelles in selective solvents offer useful solution properties. They are widely used in a variety of applications, including nanolithography,[1−3] drug delivery,[4−6] and viscosity modification.[7] The solvent quality is an important factor for both thermodynamics and dynamics of BCP micelles, which can be tuned by either changing the composition of binary solvent mixtures or altering the temperature.

In terms of thermodynamic properties, scaling models predict the aggregation number of chains within a micelle (N_{agg}) to be proportional to the interfacial tension (γ) between the core block and solvent for crew-cut micelles, which have relatively longer core than corona block lengths (i.e., $N_{core} \gg N_{corona}$).[8,9] For hairy micelles (i.e., $N_{core} \ll N_{corona}$), a scaling of $N_{agg} \sim \gamma^{6/5}$ was proposed.[10,11] Quintana and co-workers studied the structures and thermodynamic properties of micelles formed by poly(styrene)-*b*-poly(ethylene-*alt*-propylene) (PS-PEP or SEP) diblock copolymers in various solvent mixtures.[12−17] The authors reported lower aggregation numbers, smaller micelle sizes, lower critical micelle temperatures (CMT), and higher critical micelle concentrations (CMC) in less selective solvents, reflecting lower interfacial tension between the core block and solvent. Alternatively, changing the temperature is another way to adjust the solvent quality. Bang et al. showed a decrease in N_{agg} and core radius (R_{core}) of poly(styrene)-*b*-poly(isoprene) (PS-PI) micelles in tetradecane and an increase of solvent fraction in the micelle core, when the temperature was elevated toward the CMT.[18,19] Recently, Choi et al. systematically investigated a series of PS-PEP diblock copolymers in pure squalane and binary solvent mixtures of squalane and 1-phenyldodecane, where 1-phenyldodecane is a less selective solvent than squalane.[20,21] In good agreement with observations by Quintana et al. and Bang et al., the authors observed a smaller aggregation number, lower CMT, and higher solvent fraction in the core upon increasing the volume fraction of 1-phenyldodecane in binary solvent mixtures.

The solvent quality also plays a critical role in the equilibration dynamics of BCP micelles. Single-chain exchange is believed to be the dominant mechanism for BCP micelles near equilibrium.[22−24] Both theory and experiment have shown a strong dependence of chain exchange kinetics on solvent selectivity.[25−32] The scaling theory by Halperin and Alexander attributes the activation energy (E_a) of chain expulsion to the additional surface of a collapsed core block, i.e., $\gamma N_{core}^{2/3} a^2$ where γ reflects the effect of solvent selectivity, N_{core} is the number of core block repeat units, and a is the size of one repeat unit.[25,26] Following this theoretical prediction, Lund and co-workers showed an acceleration in chain

Received: September 6, 2019
Revised: December 2, 2019

DOI: 10.1021/acs.macromol.9b01877
Macromolecules XXXX, XXX, XXX−XXX

exchange kinetics of poly(ethylene-*alt*-propylene)-*b*-poly(ethylene oxide) (PEP-PEO) micelles by reducing the interfacial tension between the PEP core block and solvent, adding more *N*,*N*-dimethylformamide into water, and/or increasing temperature.[27−29] Based on kinetic studies of dilute SEP diblock copolymer micelles in squalane, Choi and co-workers established a quantitative model (eq 4) to account for the dramatic influence of the core block length, dispersity of core block length, and solvent selectivity.[30] This model attributes E_a to the unfavorable core block monomer−solvent interactions captured by $kT\chi N_{core}$, where χ is the Flory−Huggins interaction parameter between the core block and solvent. Dissipative particle dynamics (DPD) simulations by Li and Dormidontova[31] examined the effect of solvent selectivity by adjusting the pairwise repulsive interaction parameters, leading to the same form for E_a ($\sim\chi N_{core}$) as proposed by Choi et al.

However, there is a limitation to this simple relation when considering the scenario near the CMT. At T_{CMT}, there should be no energy barrier for chain expulsion, i.e., $E_a \approx 0$. However, the solvent quality is approximately at the theta condition for the core block at T_{CMT}, i.e., $\chi \approx 0.5$, taking the solvent volume as the reference volume. To address this issue, Ma and Lodge[32] proposed an elaborate χ-dependent function $f(\chi)$ to replace χ, so that the adapted expression is $E_a \sim f(\chi)N_{core}$. The authors incorporated this modified function within Choi's model and successfully interpreted the time-resolved small-angle neutron scattering (TR-SANS) data of poly(*n*-butyl methacrylate)-*b*-poly(methyl methacrylate) (PnBMA-PMMA) micelles in solvent mixtures of the ionic liquids 1-butyl-3-methylimidazolium:bis(trifluoromethylsulfonyl) imide ([BMIM][TFSI]) and 1-ethyl-3-methylimidazolium:bis-(trifluoromethylsulfonyl)imide ([EMIM][TFSI]), which are lower critical micelle temperature (LCMT) systems.

This work aims to test the universality of this χ-dependent function with SEP micelles in binary mixed solvents of squalane and 1-phenyldodecane. In contrast to the previously studied PnBMA-PMMA/ionic liquid, this system has an upper critical micellization temperature (UCMT). We quantify the consequence of varying the solvent composition and temperature on the rate of chain exchange using TR-SANS. Independent approaches, static light scattering (SLS) and cloud point measurements, have been adopted for direct measurements of χ between the core block and the solvent as a function of solvent composition and temperature.

■ EXPERIMENTAL SECTION

Materials. Two polystyrene (PS) homopolymers were synthesized by anionic polymerization. The molecular weight and molecular weight distribution of one PS with M_n = 1.3 kg/mol were characterized by matrix-assisted laser desorption/ionization mass spectroscopy (MALDI-MS), and those of the other PS (M_n = 23 kg/mol) were characterized by size exclusion chromatography equipped with a refractive index detector and a multiangle light scattering detector (SEC-MALS), as shown in Figure S1. Two pairs of SEP and core block-deuterated dSEP diblock copolymers were reproduced from the previous work.[20,30] They were synthesized by sequential anionic polymerization of PS-PI and (dPS)-PI, followed by selective saturation of the PI block using a Ni/Al catalyst under 400 psi deuterium D_2 (purchased from Cambridge Isotope Laboratories Inc.). The average repeat unit of PEP is $C_5D_{2.3}H_{7.7}$ after the deuteration reaction, where $D_{2.3}$ is a result of D_2 saturation and a small amount of H/D exchange. Perdeuterated styrene monomer (C_8D_8) was purchased from Polymer Source Inc., while pronated styrene and isoprene monomer were from Sigma-Aldrich Inc. SEC-MALS and proton nuclear magnetic resonance spectroscopy (^{1}H-NMR) were performed to determine the molecular weight and molecular weight distribution, which are summarized in Table 1. The number in the name of each polymer refers to the molecular weight, e.g., SEP 26−70 indicates $M_n \approx$ 26 and 70 kg/mol for the PS and PEP blocks, respectively.

Table 1. Polymer Characteristics[d]

polymers	$M_{n,\,PS}$[a] (kg/mol)	$M_{n,\,PEP}$[b] (kg/mol)	M_w/M_n[a]
PS 1.3	1.3[c]		1.10[c]
PS 23	23		1.03
SEP 26−70	26	70	1.04
dSEP 29−71	29	71	1.10
SEP 42−64	42	64	1.05
dSEP 47−67	47	67	1.10

[a]Determined by SEC-MALS. [b]Determined by ^{1}H NMR spectroscopy from the proton peaks of PS and PEP. [c]Determined by MALDI. [d]Note: Characteristics of SEP and dSEP diblocks were reproduced from refs 20 and 30.

Squalane (sql) was used as a highly selective solvent for the PEP blocks, so that the PS blocks aggregate into the core while PEP blocks form the swollen corona. 1-Phenyldodecane (phd), on the other hand, is relatively less selective, capable of dissolving SEP diblock polymers as free chains. Binary solvent mixtures were prepared by mixing squalane with various volume fractions of 1-phenyldodecane, which were calculated using densities of squalane (0.810 g/mL) and 1-phenyldodecane (0.856 g/mL) at room temperature, assuming no volume change on mixing. Deuterated 1-phenyldodecane ($C_{18}D_{30}$) and deuterated squalane ($C_{30}D_{62}$) used in neutron scattering experiments were purchased from CDN Isotopes Inc., while regular solvents were from Sigma-Aldrich Inc.

Micelle Solution Preparation. Dilute micelle solutions (0.5 and 1 vol %) were prepared using a co-solvent procedure. The polymer was dissolved in squalane with a similar amount of dichloromethane (Sigma-Aldrich Inc.) as co-solvent. After the polymer was completely dissolved, the solution was filtered through 0.2 μm hydrophobic PTFE filters to remove dust. The dichloromethane was then evaporated at room temperature for 2 days until a constant weight was achieved. Micelles formed as the dichloromethane were removed, due to unfavorable enthalpy of mixing between the PS block and the solvent. Micelle solutions were filtered again using 0.2 μm filters and were degassed under vacuum for 5 min to remove air bubbles and residual dichloromethane. Finally, micelle solutions were annealed at 160 °C for 1 h to equilibrate and then allowed to cool back to room temperature.

Cloud Point Measurements. The cloud point measurements were performed on a home-built optical transmission apparatus, which consists of a helium−neon laser with wavelength λ = 633 nm, a sample heating stage, and a photodiode detector. Various volume fractions of 1.3 kg/mol PS were mixed with squalane into a glass ampule, which was then flame-sealed under vacuum. The sample was heated to 180 °C or a higher temperature, held for 30 min to completely dissolve, i.e., as a one-phase solution, and followed by subsequently cooling at a rate of 1 °C/min. As shown in Figure 5a, the transmittance showed a sudden decrease when the solution underwent phase separation. The cloud point was defined as the temperature at which the transmittance dropped to 80% of the transmittance of the one-phase solution.

Static Light Scattering (SLS). SLS was performed to determine the second virial coefficient A_2 of PS in pure squalane and in binary solvent mixtures of squalane and 1-phenyldodecane. A series of dilute PS (M_n = 23 kg/mol, M_w/M_n = 1.03, in Table 1) solutions with various concentrations (10−50 mg/mL) were prepared in binary mixed solvents and sealed in LS glass tubes. The refractive indices of the solvent and the refractive index increment (dn/dc) values for the

DOI: 10.1021/acs.macromol.9b01877
Macromolecules XXXX, XXX, XXX−XXX

dilute PS solutions were measured using a refractometer operated with red light (≈650 nm), as shown in Figure S2. The dashed lines gave the dn/dc value, 0.0989 mL/g, which was almost independent of temperature in the range of 23−60 °C, as shown in Figure S3a. These samples were investigated using a Brookhaven BI-200SM goniometer and laser light scattering system with λ = 637 nm. The instrument constant was calibrated using toluene at 23 °C. Measurements were taken at multiple angles θ ranging from 50 to 130° in 10° increments, leading to a range of scattering vector $q = 4\pi n \sin(\theta/2)/\lambda$ from 0.012 to 0.026 nm^{-1}. Figure S3b gives an example of obtaining the second virial coefficient A_2 of dilute PS solutions in 1-phenyldodecane from a Zimm plot, where R_θ is the Rayleigh ratio in units of cm^{-1}, K is a constant, θ is the scattering angle, and c is the polymer concentration. Kc/R_θ was independent of the scattering angle because this polymer is rather small ($R_g \approx 4$ nm in a θ solvent), $qR_g \leq 0.1$, while Kc/R_θ decreased with increasing polymer concentration. The second virial coefficient $A_2 = (-1.7 \pm 0.1) \times 10^{-4}$ cm^3 mol/g^2 was obtained from the slope of Kc/R_θ vs c, indicating that 1-phenyldodecane is a poor solvent for PS at 23 °C.

Dynamic Light Scattering (DLS). High-temperature DLS measurements were performed on a home-built light scattering instrument with a laser wavelength λ = 488 nm using silicon oil as an index matching fluid. A temperature ramp was designed for micelle samples to determine the critical micelle temperature (T_{CMT}), at which micelles dissolve into free chains, causing a drop in both scattering intensity and hydrodynamic radius. The scattering intensity is proportional to the molecular weight of the micelles $M_{w,mic}$ at $T < T_{CMT}$ or the free polymers $M_{w,p}$ at $T > T_{CMT}$. Therefore, the intensity changes by a factor of ca. N_{agg} across the T_{CMT}. Figure S4 shows the temperature-dependent response of a 0.5 vol % SEP 26−70 diblock polymer solution in the 25/75 vol % 1-phenyldodecane/squalane mixing solvent upon heating (red curve) and cooling (blue curve). At each temperature, the sample was held for 10 min to thermally equilibrate. T_{CMT} is estimated to be around 130 °C. When the temperature traversed T_{CMT}, about 2 orders of magnitude change was observed in the detector counts, as shown in Figure S4a. Simultaneously, the apparent R_h value drops from 37 to 5 nm (Figure S4b). This change is fully reversible as the cooling curve overlaps with the heating curve.

Small-Angle X-ray Scattering (SAXS). SAXS was performed at the 5-ID-D beamline at the DuPont-Northwestern-Dow (DND-CAT) station at Argonne National Laboratory. A beam energy of 17 keV, corresponding to a wavelength 0.73 Å, and a sample-to-detector distance of 8.5 m were selected to give a q range of 0.003−0.15 $Å^{-1}$. Micelle solutions were loaded into capillary tubes and fixed onto a multiposition capillary stage for heating and cooling. At each temperature, samples were annealed for 10 min to equilibrate thermally, and then exposed to X-rays for 1 s. A pure solvent sample was measured as a background and subtracted from micelle solution scattering. Since micelle samples are isotropic, two-dimensional scattering images were azimuthally averaged to one-dimensional intensity $I(q)$ vs q in arbitrary intensity units.

Figure S5 shows the SAXS patterns of 1 vol % SEP 26−70 micelles in the 25/75 vol % 1-phenyldodecane/squalane binary mixed solvent after the solvent background was subtracted. Low-temperature scattering patterns show a distinct micelle form factor at high q with the first minimum q_1 = 0.051 $Å^{-1}$ and a small bump in the structure factor at low q (≈ 0.007 $Å^{-1}$) reflecting intermicelle interactions. Based on the first minimum appearing at q_1 = 0.051 $Å^{-1}$, the micelle core radius R_{core} is estimated to be 8.8 nm at 25 °C by applying the characteristic equation for the minima in the hard-sphere form factor, i.e., $qR_{core} = 4.49$. The red lines in the figure are the best fits to the hard-sphere model developed for BCP micelles by Pedersen et al.[33−37] The model fits give R_{core} = 8.8 nm with a standard deviation of core radii σ_{Rc} = 0.7 nm, in good agreement with the calculated results from the first minimum. However, more solvent penetrates into the core, leading to less contrast between the micelle core and solvent, as evidenced by weaker first minima in the SAXS patterns with increasing temperature. Micelle features disappeared at 150 °C, indicating that no micelles present at this temperature. The T_{CMT} is, therefore, within the temperature window of 120−150 °C, which is consistent with DLS results (≈130 °C).

Time-Resolved Small-Angle Neutron Scattering. TR-SANS experiments were conducted on the CG-2 SANS beamline in the High Flux Isotope Reactor (HFIR), Oak Ridge National Laboratory. We used a wavelength of 4.75 Å with the spread of $\Delta\lambda/\lambda$ = 0.13 and sample-to-detector distance of 10 m to access a q range of 0.007−0.1 $Å^{-1}$. Micelle solutions were loaded into 1 mm quartz banjo cells and fixed in a sample block for heating and cooling. Each scattering measurement takes 5 min. The evolution of excess scattering intensity is proportional to the change of contrast between the micelle cores and solvent: $I(t) - I(\infty) \sim (\rho_{core}(t) - \rho_{solvent})^2$, where $I(t)$ is the instantaneous intensity at time t,$I(\infty)$ is the intensity at infinite time (i.e., completely exchanged state), and ρ_{core} and $\rho_{solvent}$ are the scattering length densities of the core block and solvent, respectively.

A contrast matching strategy is employed for the solvent used in TR-SANS experiments, such that the scattering density of the solvent matches that of completely mixed micelle cores. $\rho_{solvent} = \rho_{core}(t = \infty) = (\rho_{hPS} + \rho_{dPS})/2 = 3.93 \times 10^{10}$ cm^{-2}, using the values listed in Table 2. Isotopic solvent mixtures of h-(1-phenyldodecane), d-(1-phenyldodecane) h-squalane, and d-squalane were prepared using the calculated volume fractions, as listed in Table 2.

Table 2. Volume Fraction of Each Component in the Contrast Matching Solvent

contrast matching solvents	h-phd	d-phd	h-sql	d-sql
50/50 vol % phd/sql	45 vol %	5 vol %	0	50 vol %
25/75 vol % phd/sql	25 vol %	0	19 vol %	56 vol %
0/100 vol % phd/sql	0	0	42 vol %	58 vol %

RESULTS AND DISCUSSION

Micelle Chain Exchange Kinetics. TR-SANS experiments were performed to probe the chain exchange kinetics of SEP block copolymer micelles in various solvent mixtures. Figure 1a shows a representative plot of time-dependent scattering intensities of 1 vol % SEP 26−70 micelles in the mixed solvent 25/75 vol % phd/sql at 58 °C. The intensity of a postmixed specimen (red curve) was measured at room temperature where no chain exchange occurs, so it represents the initial state with unmixed cores, i.e., $I(0) = I_{postmixed}$. It shows the highest intensity because of the largest contrast between micelle cores and solvent. After the system was heated to the target temperature, 58 °C, for example, micelles underwent chain exchange. Thus, the contrast between partially mixed cores and solvent decreases, leading to a decrease in scattering intensity with time, as shown in Figure 1a. The premixed micelle solution represents the state of complete chain exchange, i.e., $I(\infty) = I_{premixed}$, since the protonated and deuterated polymer chains were molecularly mixed in the micelle preparation step. Under the contrast matching condition for fully mixed cores, the intensity of the premixed specimen matches that of the solvent except in the low q regime (<0.015 $Å^{-1}$), where there is a small contribution from the corona scattering. This well-matched contrast between the core and solvent indicates that the composition of solvent molecules in the core is close to that of the macroscopic solvent mixture, due to the fact that 1-phenyldodecane and squalane are both poor solvents ($\chi_{PS\text{-}phd}$ = 0.74 and $\chi_{PS\text{-}sql}$ = 1.67, see below), leading to a low degree of overall solvation.

A normalized relaxation function, $R(t)$, is defined to quantify the rate of chain exchange

DOI: 10.1021/acs.macromol.9b01877
Macromolecules XXXX, XXX, XXX−XXX

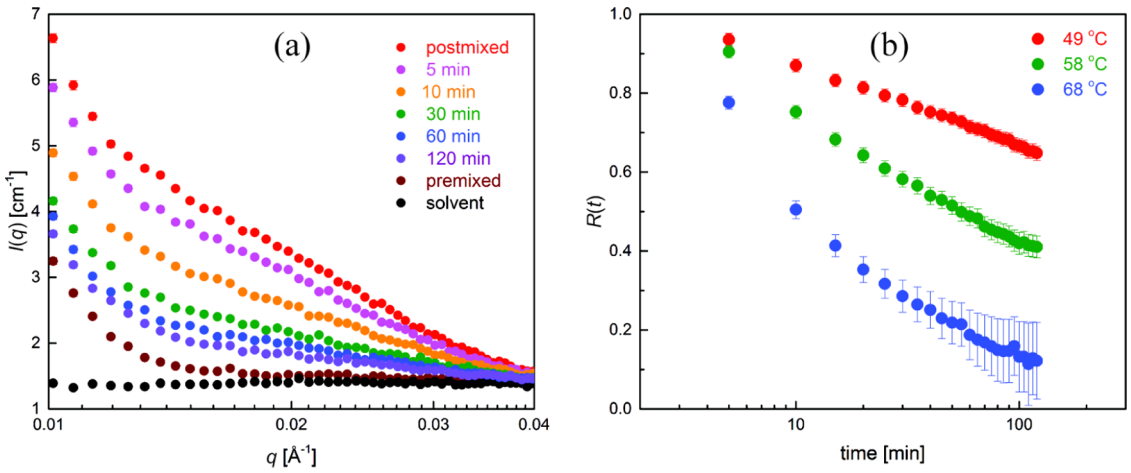

Figure 1. (a) Representative TR-SANS intensity evolution traces at 58 °C and (b) $R(t)$ traces of the 1 vol % SEP 26−70 micelles in the 25/75 vol % phd/sql solvent at different temperatures.

$$R(t) = \sqrt{\frac{I(t) - I(\infty)}{I(0) - I(\infty)}} \tag{1}$$

where $I(0)$, $I(t)$, $I(\infty)$ are the intensities at $t = 0$, at time t, and at infinite time, respectively. The values of scattering intensities are integrated over the q range 0.01−0.04 Å^{-1}. As shown in Figure 1b, $R(t)$ decays more rapidly at higher temperatures, which reflects faster chain exchange kinetics. The error bars of $R(t)$ in Figure 1b are propagated from the errors in the intensities, given by

$$\delta R(t) = \sqrt{\left[\frac{\partial R(t)}{\partial I(t)}\delta I(t)\right]^2 + \left[\frac{\partial R(t)}{\partial I(\infty)}\delta I(\infty)\right]^2 + \left[\frac{\partial R(t)}{\partial I(0)}\delta I(0)\right]^2} \tag{2}$$

where $\delta I(t)$, $\delta I(\infty)$, and $\delta I(0)$ are uncertainties in the measured values of $I(t)$, $I(\infty)$, and $I(0)$, respectively. $\delta I(t)$, $\delta I(\infty)$, and $\delta I(0)$ were integrated over the same q range of 0.01−0.04 Å^{-1}. As shown in Figure 1b, the propagated errors of $R(t)$ became larger at higher temperatures and longer relaxation times, e.g., at 68 °C and 100 min.

The time−temperature superposition (tTS) method is employed to construct $R(t)$ master curves with a reference temperature of 70 °C, as shown in Figure 2. The chain exchange rate increases significantly for both SEP micelle systems with reducing solvent selectivity by mixing squalane with a higher volume fraction of 1-phenyldodecane. For instance, SEP 42−64 micelles exchange chains about 10^5 times faster in 50 vol % squalane than in 75 vol % squalane and, furthermore, 10^{10} times faster than in pure squalane. The same trend was observed for SEP 26−70 micelles. The timescale of chain exchange is prohibitively large in pure squalane, i.e., ≈10^5 and 10^8 min at $R(t) = 0.5$ for SEP 26−70 and SEP 42−64 micelles, respectively. The main reason is that the reference temperature 70 °C is close to the glass transition temperature (T_g) of the PS block in the micelle core,[41] where the PS chains are almost frozen.

The empirical shift factors used in the tTS method are displayed in Figure 3. We note that the shift factors of previously studied micelle systems in pure squalane have been converted from the reported values because the reference temperature was switched from 125 to 70 °C. Since the T_g of

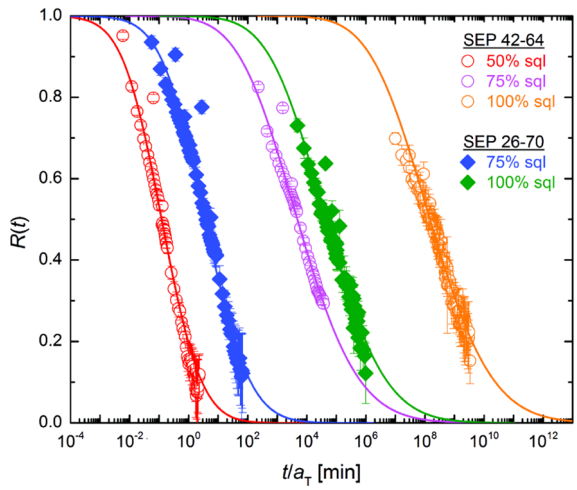

Figure 2. $R(t)$ master curves and theoretical model fits for 1 vol % SEP micelles in various binary mixed solvents at a reference temperature of 70 °C, where the volume fraction of squalane in binary mixed solvents varied from 50 to 100%. Data of SEP micelles in pure squalane were adapted from ref 30.

the PS block in the core is about 70 °C for micelles in pure squalane,[41] the previous empirical trend line should still work but needs shifting to the reference temperature 70 °C, i.e., $\log(a_T) = -0.0936 \times (T - 70\ °C)$. The data of binary mixed solvents at multiple temperatures are displayed in Figure S6 in the Supporting Information and were empirically shifted to overlap with those obtained at 70 °C, e.g., data of SEP 26−70 in the 25/75 vol % phd/sql solvent, which were collected at 68 °C.

The T_g of the core block in binary mixed solvents will decrease with the increase of the solvent fraction in the core region when the solvent selectivity is reduced. The values of the reduced core T_g are estimated by the Fox equation[42]

$$\frac{1}{T_{g,PS}^{wet}} = \frac{1 - w_1 - w_2}{T_{g,PS}^{dry}} + \frac{w_1}{T_{g,sql}} + \frac{w_2}{T_{g,phd}} \tag{3}$$

where T_g^{wet} is the glass transition temperature of the core block in a wet core with weight fractions w_1 and w_2 of squalane (sql) and 1-phenyldodecane (phd), respectively. $T_g^{dry} \approx 343$ K (70 °C) represents the glass transition temperature of a dry core as

DOI: 10.1021/acs.macromol.9b01877
Macromolecules XXXX, XXX, XXX−XXX

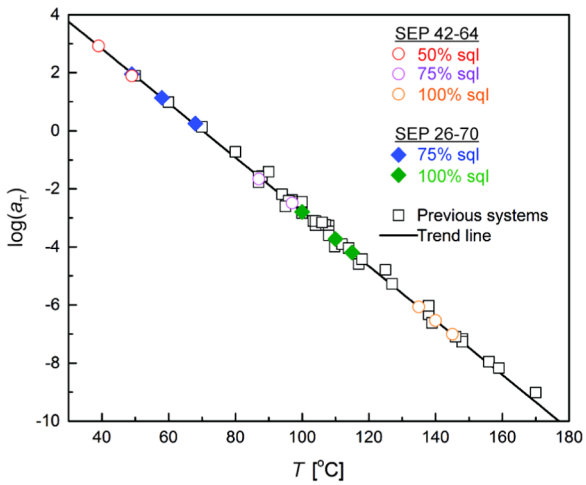

Figure 3. Shift factors $\log(a_T)$ and the trend line as a function of temperature at a reference temperature of 70 °C, open circles for SEP 42−64, and filled diamonds for SEP 26−70 in binary mixed solvents, together with the shift factors and the fitted trend line from our previous studies: $\log(a_T) = -0.0936 \times (T - 70\ °C)$.[30,38−40,47]

reported by Lai et al.[41] This value is lower than T_g of bulk PS due to the small size of the PS domains in the spherical micelles (≤11 nm) and because the PS core block repeat units located at the interface are plasticized by the solvent. Solvent glass transition temperatures $T_{g,sql} \approx 168$ K and $T_{g,phd} \approx 180$ K were obtained from the literature.[43−45] Here, we note that no residual solvent was detected in the core of SEP micelles in squalane at 70 °C by Choi et al. (which was more than 130 °C lower than the critical micelle temperature T_{CMT}), based on SAXS and SANS measurements.[20] Bang et al. also showed no solvent in the core of PS-PI micelles in tetradecane at temperatures of 40 °C or more below T_{CMT}.[18] We calculated T_g^{wet} assuming that the core composition is the same as the overall solvent composition (see above) using the volume fraction of binary mixed solvent in the core reported by Choi et al.[20,21] and listed in Table 3. The estimated T_g for the slightly solvated PS core would not change significantly with small variations in solvent composition due to the similar T_g values of squalane and 1-phenyldodecane. For example, 13 vol % solvent is observed for the SEP 42−64 micelle in 25/75 vol % phd/sql binary solvent. In this case, the weight fractions of PS, squalane, and 1-phenyldodecane are estimated to be 89, 3, and 8 wt % in the core region, respectively. The glass transition temperature of the PS core block in such a wet core is estimated to be 37 °C by eq 3. As the solvent selectivity decreases, more solvent penetrates into the core, leading to a lower T_g of the PS block, as shown in Table 3. Note that $T_{g,PS}$ in SEP 26−70 micelle cores is assumed to be the same as SEP 42−64 micelles in the same binary solvent because the molecular weight dependence of T_g is weak in this molecular weight range.[46] Here, we note that a constant solvent fraction in the core is assumed for the micelles at the TR-SANS experimental temperatures, which are at least 50 °C lower than the corresponding T_{CMT}. Since the reference temperature of 70 °C is also well below T_{CMT}, the core should contain a similar amount of solvent as at the experimental temperatures, which we exploit in generating the TR-SANS master curves.

As noted in Table 3, the TR-SANS experimental temperatures were designed for appropriate timescales from several minutes to hours, to capture the evolution of scattering intensities by SANS. These temperatures are at least 12 °C higher than the glass transition temperature of the core block, so that the core blocks are able to relax. On the other hand, they are more than 50 °C lower than the critical micelle temperature where the rate of chain exchange would be very fast.

To describe the TR-SANS data quantitatively, a theoretical model (eq 4) has been established by previous studies on SEP diblock micelles.[30,47] This model makes the following assumptions: (i) single-chain exchange is the dominant mechanism near equilibrium; (ii) chain expulsion is the rate-limiting step; (iii) the motion of core blocks follows Rouse dynamics when buried in the micelle cores; and (iv) the activation energy E_a of chain expulsion is a result of the enthalpy penalty from unfavorable interactions between the core blocks and corona/solvent matrix and the entropy gain from the relief of corona chain stretching upon expulsion.

$$R(t) = \int P(N_{core}) \exp\left[-t \frac{6\pi^2 kT}{N_{core}^2 b^2 \zeta} \exp\left(-f(\chi) N_{core} + \frac{3}{2} s_{corona}^2\right)\right] dN_{core} \quad (4)$$

$$P(N_i) = \frac{z^{z+1}}{\Gamma(z+1)} \frac{N_i^{z-1}}{N_n^z} \exp\left(-\frac{z N_i}{N_n}\right) \quad (5)$$

Here, N_{core} is the degree of polymerization of the core blocks and $P(N_{core})$ is a Schulz−Zimm distribution function that accounts for dispersity of the core blocks, given by eq 5, where $z = [N_w/N_n - 1]^{-1}$, Γ is the γ function, and N_w/N_n represents the dispersity. Considering the small mismatch in the

Table 3. Characteristics of SEP Micelles in Binary Mixed Solvents[h]

micelle systems	R_h[a−d] (nm)	N_{agg}[a−d]	R_{core}[a−d] (nm)	f_{sol}[a−d]	$T_{g,PS}$[e] (°C)	T_{CMT}[f] (°C)	$T_{TR\text{-}SANS}$[g] (°C)
SEP 42−64 micelles in							
50/50 vol % phd/sql	34	53	10.1	≈0.21	≈20	110	39−49
25/75 vol % phd/sql	35	72	10.9	≈0.13	≈37	180	87−97
0/100 vol % phd/sql	43	83	11.0	≈0	≈70	>200	135−145
SEP 26−70 micelles in							
25/75 vol % phd/sql	35	62	8.8	≈0.13	≈37	130	49−68
0/100 vol % phd/sql	43	71	8.9	≈0	≈70	≈200	100−115

[a−d]Micelle core radius, aggregation number of chains within a micelle, hydrodynamic radius, and volume fraction of solvent in the micelle core at 70 °C. [e]The glass transition of the PS core block in the core estimated by the Fox equation. [f]The critical micelle temperature determined by dynamic light scattering (DLS). [g]The temperatures carried out in TR-SANS experiments. [h]Note that f_{sol}, N_{agg}, R_{core}, R_h, and T_{CMT} data were reproduced from the previous work,[20,21] except those of SEP 26−70 micelles in 25/75 vol % phd/sql, as shown in Figures S4 and S5.

DOI: 10.1021/acs.macromol.9b01877
Macromolecules XXXX, XXX, XXX−XXX

Table 4. Parameters Used in the Model

micelle systems	$\langle N_{core}\rangle$	$\zeta_{T = 70°C}$ (N s/m)	s_{corona}	$f(\chi)^{fitted}$	N_w/N_n^{fitted}
SEP 42−64 micelles in					
50/50 vol % phd/sql	412	3.08×10^{-8}	1.22	2.34×10^{-2}	1.02
25/75 vol % phd/sql	412	3.53×10^{-7}	1.23	4.32×10^{-2}	1.04
0/100 vol % phd/sql	412	1.20×10^{-3}	1.66	5.33×10^{-2}	1.04
SEP 26−70 micelles in					
25/75 vol % phd/sql	255	3.53×10^{-7}	1.28	4.59×10^{-2}	1.02
0/100 vol % phd/sql	255	1.20×10^{-3}	1.68	5.89×10^{-2}	1.04

molecular weight of PS and dPS blocks from the isotopic pair of SEP and dSEP diblock copolymers, the SEP 26−40/dSEP 29−71 system has an average $\langle N_{core}\rangle = 255$, while SEP 42−64/dSEP 47−67 has $\langle N_{core}\rangle = 412$. N_w/N_n is taken as a fitting parameter to depict the slope of $R(t)$, as listed in Table 4.

The first term inside the first exponential term, $N_{core}^2 b^2 \zeta / 6\pi^2 kT$, represents the longest Rouse relaxation mode for the core blocks, where k is Boltzmann's constant, $T = 343$ K (70 °C) is the temperature, ζ is the monomeric friction factor, and $b = 0.67$ nm is the statistical segment length of the core block. We assume that 26 and 42 kg/mol PS are not, or at most weakly, entangled. The friction factor ζ is a strong temperature-dependent function described by the Williams−Landel−Ferry (WLF) equation.[48]

$$\log\left(\frac{\zeta_T}{\zeta_g}\right) = -\frac{C_1^g(T - T_g)}{C_2^g + (T - T_g)} \tag{6}$$

where $\zeta_g = 1.2 \times 10^{-3}$ N s/m is the monomeric friction factor at T_g and $C_1^g = 11.0$ and $C_2^g = 69.8$ °C are two empirical constants, which are obtained from the rheological data of the bulk PS homopolymer.[49] Since the T_g of PS in the micelle core varies with solvent composition, values of ζ at the reference temperature of 70 °C are calculated by eq 6 for various binary mixed solvents. As listed in Table 4, ζ is more than 3 orders of magnitude lower with only 13 vol % solvent present in the core for micelles in the solvent of 75 vol % squalane, than in pure squalane. This decrease in ζ significantly facilitates the movement of core blocks and, thus, accelerates the kinetics of chain exchange.

The energy barrier for chain expulsion is expressed in the exponential term, where $f(\chi)$ is a χ-dependent function where χ represents the Flory−Huggins interaction parameter between the core block and solvent. Choi et al. originally took the enthalpy part to be $\alpha\chi N_{core}$, where α is a prefactor of order unity.[30] Here, $f(\chi)$ is adopted as a fitting function, and the fitted results in Table 4 will be discussed with χ values obtained from SLS and cloud point measurements (see below). The entropic term arises from the increase in corona chain conformations after the polymer chain escapes from the micelle into solvent.[47] Assuming that the corona chains follow Gaussian chain statistics,[50] the corona chain stretching parameter (s_{corona}) is defined as $s_{corona} = R_g/R_{g,0}$, where R_g is the radius of gyration of corona chains in the micelle and $R_{g,0}$ is the unperturbed value neglecting the excluded volume effect of PEP corona blocks in squalane.[51] R_g is estimated to be half of corona layer thickness (L_{corona}), i.e., $R_g = L_{corona}/2 = (R_h - R_{core})/2$, where R_h is the micelle hydrodynamic radius determined by DLS, as shown in Figure S4b, and R_{core} is the core radius characterized by SAXS, as demonstrated in Figure S5. These data were summarized in Table 3. $R_{g,0}$ is calculated by $R_{g,0} = 0.0392M^{1/2}$ ($R_{g,0}$ in unit of nm) at 298 K[52] with M = 70000 and 64000 for SEP 26−70 and SEP 42−64 micelles, respectively. As listed in Table 4, s_{corona} decreases with reduced solvent selectivity. This is attributed to less crowding of corona chains as the aggregation number decreases in a less selective solvent. We note that the mixing entropy (ΔS) of the core blocks and solvent is negligible for the SEP micelles compared to the core−solvent interaction and corona stretching energy in eq 4. Lund et al. considered the impact of mixing entropy in the core of PS-PB (10−10 kg/mol) micelles in n-alkanes, where the core contained 39−54 vol % solvent.[54] However, the SEP micelles considered here have much less solvent (0−21 vol %) in the core due to the longer core block lengths (N_{PS} = 255 and 412 for SEP 26−70 and SEP 42−64, respectively) and higher χ (χ = 1.24−1.67, as listed in Table 5).

Table 5. Enthalpic Interactions between the Core Block and Solvent[a]

micelle systems	χ' ($v_0 = v_1$)	χ ($v_0 = v_2$)	$a(\chi - v_2/v_1)\langle N_{core}\rangle$	$f(\chi)\langle N_{core}\rangle$
SEP 42−64 micelles in				
50/50 vol % phd/sql	1.24	0.238	5.4	9.6
25/75 vol % phd/sql	1.46	0.279	15.1	17.8
0/100 vol % phd/sql	1.67	0.320	25.0	22.0
SEP 26−70 micelles in				
25/75 vol % phd/sql	1.46	0.279	9.3	11.7
0/100 vol % phd/sql	1.67	0.320	15.5	15.0

[a]Note that $a = 0.58$ gives best fit between $a(\chi - v_2/v_1)\langle N_{core}\rangle$ and $f(\chi)\langle N_{core}\rangle$, where $v_1 = 463.5$ cm^3/mol and $v_2 = 100$ cm^3/mol are molar volumes of solvent and PS repeat unit, respectively.

Table 4 summarizes the parameters used in this theoretical model and two adjustable fitting parameters, i.e., $f(\chi)$ and N_w/N_n. The solid lines in Figure 2 represent best fits to the TR-SANS data. The fitted N_w/N_n values are consistent with anionically polymerized PS core blocks with a narrow dispersity. They are smaller than the apparent dispersity of the corresponding SEP diblock copolymers (M_w/M_n) obtained from SEC measurements (Table 1). This is attributed to the well-known broadening effect in SEC for narrow distribution polymers.[55] The fitted $f(\chi)$ values decrease by more than a factor of two by decreasing the volume fraction of squalane in binary mixed solvents. This effect results from the reduced enthalpy of mixing between the core block and solvent. On the other hand, for a given solvent composition, $f(\chi)$ values are almost independent of the molecular characteristics of SEP block copolymers. We next estimate χ using SLS and cloud points measurements as a function of solvent composition and temperature. Thus, a more exact dependence of the barrier on χ can be obtained, i.e., for the function $f(\chi)$.

Role of χ. Figure 4a summarizes the second virial coefficients obtained from SLS measurements. A_2 increases

DOI: 10.1021/acs.macromol.9b01877
Macromolecules XXXX, XXX, XXX−XXX

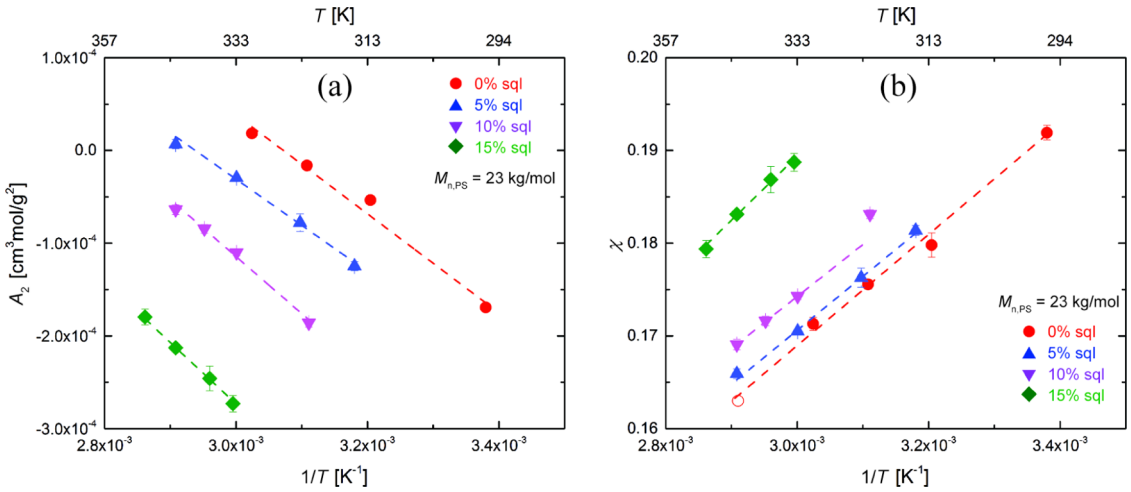

Figure 4. (a) Second virial coefficient (A_2) for PS in binary mixed solvents as a function of temperature and composition and (b) calculated χ values from A_2, taking the PS repeat unit volume as the reference volume. The open circle is an extrapolation to 70 °C.

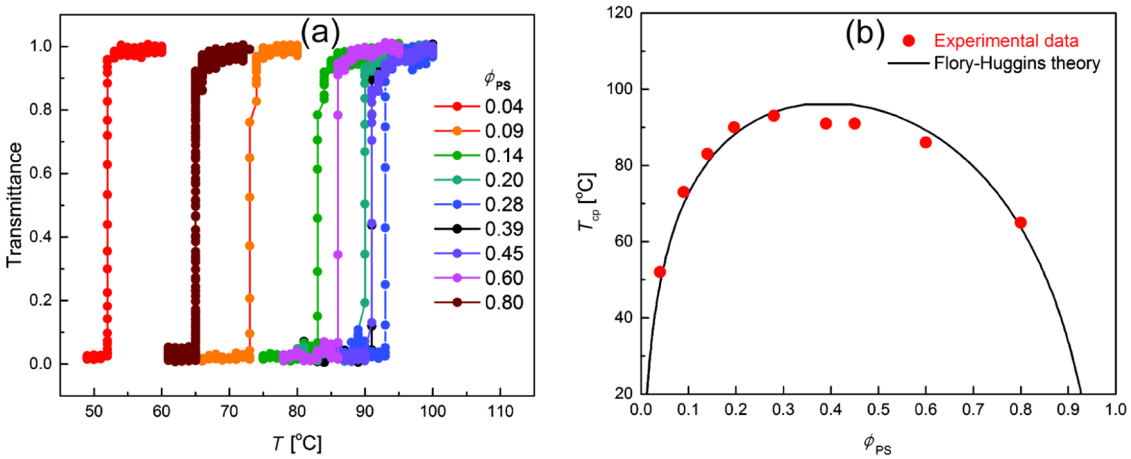

Figure 5. (a) Temperature-dependent transmittance of PS solutions in squalane at different PS volume fractions and (b) cloud points and the coexistence curve calculated by the Flory−Huggins theory with $\chi = 287/T - 0.517$.

with increasing temperature, indicating higher solubility of PS in the solvent, which is an upper critical solution temperature (UCST) system. On the other hand, A_2 is strongly dependent on the solvent composition as well, decreasing with the increasing volume fraction of squalane (ϕ_{sql}).

$$\chi' = \frac{1}{2} - \rho_p^2 v_1 A_2 \ (v_0 = v_1) \tag{7}$$

$$\chi = \frac{v_2}{v_1}\chi' \ (v_0 = v_2) \tag{8}$$

Applying the Flory−Huggins theory for dilute polymer solutions, χ values were calculated from A_2 by eq 7 and then converted by eq 8 taking the molar volume of the PS repeat unit (v_2 = 100 cm^3/mol) as the reference volume v_0, instead of the molar volume of the solvent v_1 in the traditional definition, where ρ_p = 1.04 g/cm^3 is the density of PS. This is due to the use of the chemical degree of polymerization in the fitting model (eq 4) for TR-SANS data, i.e., $N_2 = N_{core}$ only if $v_0 = v_2$, where N_2 represents the volumetric degree of polymerization of the PS block. Moreover, the values of χ were determined in binary mixed solvents of low squalane volume fraction ϕ_{sql} (= 0, 5, 10, and 15 vol %), whereas TR-SANS experiments were performed in the other extreme, i.e., ϕ_{sql} = 50, 75, and 100 vol %. It is mathematically convenient to extrapolate χ to high ϕ_{sql} solvents using a constant reference volume since v_1 varies with solvent composition. If a linear relationship is assumed with v_1 = 288 and 522 cm^3/mol for 1-phenyldodecane and squalane, respectively, v_1 = 288 + 234ϕ_{sql} cm^3/mol is estimated for binary mixed solvents. As summarized in Figure 4b, χ decreases with increasing temperature, following the empirical relation $\chi = A/T + B$. The slope of χ vs $1/T$ was observed to be a weak function of solvent composition in this relatively narrow composition range, while the intercept showed appreciable changes due to different excess entropy of mixing.

Considering the uncertainty in extrapolation of χ vs solvent composition, optical transmittance experiments were performed to measure cloud points of PS solutions in squalane, and, thus, to determine χ between PS and pure squalane. A lower-molecular-weight PS (M_n = 1.3 kg/mol, M_w/M_n = 1.1) was used to obtain accessible cloud points. We, therefore, assume that any M dependence of χ is less important than the dependence on solvent composition. Figure 5a displays the temperature-dependent transmittance of PS solutions. The cloud point was defined as the temperature at which the transmittance dropped to 80% of the transmittance of the one-phase solution. Figure 5b summarizes cloud points of PS solutions at different PS volume fractions (ϕ_{PS}), ranging from

DOI: 10.1021/acs.macromol.9b01877
Macromolecules XXXX, XXX, XXX−XXX

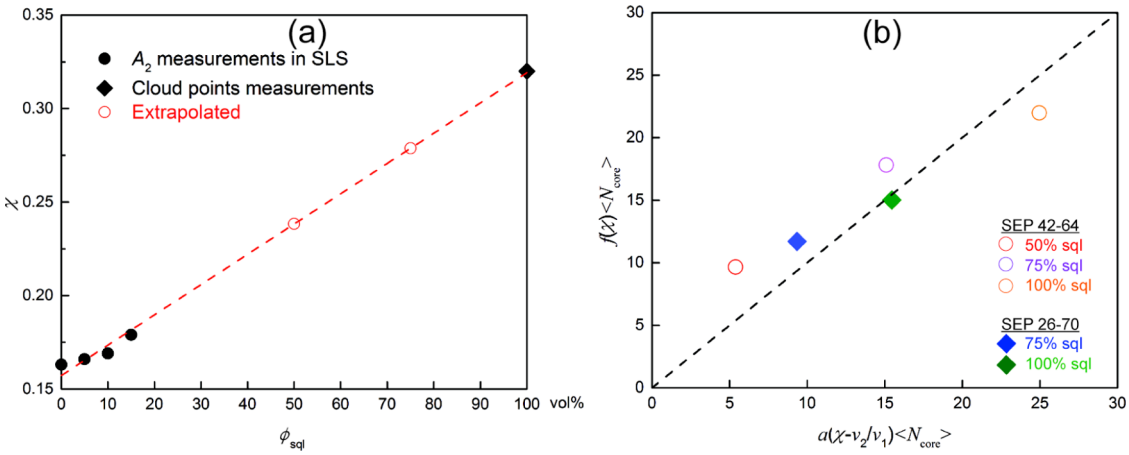

Figure 6. (a) χ values (black circles and diamonds) between PS and binary mixed solvents as a function of composition at 70 °C and interpolated values at ϕ_{sql} = 50 and 75 vol % (red circles) and (b) enthalpy penalty of chain expulsion for SEP micelles in binary mixed solvents, comparing the fitted results from TR-SANS ($f(\chi)\langle N_{core}\rangle$) and calculated values by the Flory−Huggins theory ($a(\chi - v_2/v_1)\langle N_{core}\rangle$).

0.04 to 0.8. The black line was the coexistence curve calculated by the Flory−Huggins theory, with two adjustable parameters in χ, assuming $\chi = A/T + B$. Here, the reference volume is $v_0 = v_2$ = 100 cm^3/mol, and N_1 = 5.2 and N_2 =12.5 are volumetric degrees of polymerization for squalane and 1.3 kg/mol PS, respectively. As shown in Figure 5b, $\chi = 287/T - 0.517$ gives the best fit. Therefore, χ = 0.32 between PS and squalane at 70 °C, with $v_0 = v_2$ = 100 cm^3/mol, i.e., χ' = 1.67 if converted with $v_0 = v_1$ = 522 cm^3/mol. This large quantity suggests the strong incompatibility between PS core blocks and the solvent, driving the segregation of PS blocks into micelle cores.

Figure 6a displays χ between PS and binary mixed solvents of various ϕ_{sql} at 70 °C, where the data of ϕ_{sql} = 0, 5, 10, and 15 vol % were determined from A_2 measurements in SLS, ϕ_{sql} = 100 vol % was determined by cloud point measurements, and ϕ_{sql} = 50 and 75 vol % were obtained from the linear fitting between χ and ϕ_{sql}. We assume that the molecular weight dependence of χ is negligible in the range of 26−42 kg/mol. Consistent with this, Hoarfrost and co-workers showed that χ between PnBMA and the ionic liquids [BMIM][TFSI] and [EMIM][TFSI] was almost constant when varying the molecular weight of PnBMA from 25 to 115 kg/mol.[53]

$$\Delta E/kT = a\left(\chi - \frac{v_2}{v_1}\right)N_{core}\ (v_0 = v_2) \tag{9}$$

Ma and Lodge[32] derived the energy barrier of chain expulsion by the free energy difference (ΔE) between the core block within the micelle cores and in the solvent from the Flory−Huggins theory, as given by eq 9, where $v_0 = v_2$ and a is a constant. In their description, the micelle solution was treated as a two-phase system that is under equilibrium, with a polymer-rich phase within the micelle cores and a solvent-rich phase outside. For simplicity, the entropic contribution of the corona blocks was neglected in the derivation. Therefore, ΔE purely represents the enthalpic penalty from unfavorable core block monomer−solvent contacts. Figure 6b shows the enthalpy penalty of chain expulsion for SEP micelles in binary mixed solvents. The fitted results from TR-SANS (i.e., $f(\chi)\langle N_{core}\rangle$) agree with the calculated values within 4 kT difference, i.e., $a(\chi - v_2/v_1)\langle N_{core}\rangle$, where a = 0.58, v_1 = 463.5 cm^3/mol and v_2 = 100 cm^3/mol were used in the calculation. The validation of this χ-related expression is independent of the molecular characteristics for the two SEP block copolymers with $\langle N_{core}\rangle$ that differ by a factor of 1.6, for which the exchange rate differs by a factor of 3−4 orders of magnitude.

A relatively large difference in fitted vs calculated values (5.4 vs 9.6) arises for the 50/50 vol % phd/sql micelle system in Table 5. This discrepancy is attributed to the two strict assumptions in the derivation of eq 9, that the solvent fraction in the core is close to zero and that polymer fraction in the solvent is negligible. They are reasonable assumptions for SEP micelles in pure squalane, where the micelle core is dry[20] and the CMC is estimated to be as low as 10^{-6} g/mL.[12] However, about 21 vol % solvent remains within the cores for 50 vol % squalane, as shown in Table 3. More solvent will penetrate into the core if χ between the core block and solvent is further reduced. Similarly, the significant drop in the CMT of SEP micelles reflects an increase of CMC in less selective solvents. Therefore, it is risky to neglect the polymer concentration in the solvent for SEP 42−64 micelles in 50/50 vol % phd/sql, which potentially causing the deviation from the theory. In this case, where χ is not large enough, a more complicated χ-dependent function is probably needed to account for the offset.

Summary. The chain exchange kinetics of SEP block copolymer micelles was investigated in pure squalane and in binary solvent mixtures of squalane and 1-phenyldodecane by TR-SANS. The solvent composition significantly influences the kinetics of chain exchange between micelles, where 5 orders of magnitude faster kinetics were observed when mixing squalane with only 25 vol % 1-phenyldodecane. This acceleration in the kinetics is attributed to two primary factors: (i) faster motion of core blocks in the core as more solvent penetrates into the core, serving as a plasticizer and (ii) reduced energy barrier of chain expulsion due to the higher solubility between the core block and solvent. By fitting the TR-SANS data to a theoretical model, the enthalpic penalty of chain expulsion was determined for SEP micelles in various binary mixed solvents, reflecting the change of the Flory−Huggins interaction parameter χ between the core block and solvent. Previously, Ma and Lodge proposed a χ-dependent function for this energy barrier in a strong segregated micelle system based on the Flory−Huggins theory. With a direct measurement of χ between the PS core block and solvent from second virial coefficients by SLS and from cloud point measurements by

DOI: 10.1021/acs.macromol.9b01877
Macromolecules XXXX, XXX, XXX−XXX

optical transmittance, the theoretically predicted values of activation energy compare favorably with the experimental results obtained from TR-SANS. In summary, this work quantifies the role of χ in the kinetics of chain exchange for a UCMT micelle system. The successful interpretation of chain exchange kinetics in both PnBMA-PMMA/ionic liquids and SEP/hydrocarbon solvents points toward the possible universality of this χ-dependent function for the activation energy. This potentially provides insights in selecting an appropriate solvent for the design of micelles.

■ ASSOCIATED CONTENT

Supporting Information

The Supporting Information is available free of charge at https://pubs.acs.org/doi/10.1021/acs.macromol.9b01877.

(i) MALDI-MS of 1.3 kg/mol PS and SEC trace of 23 kg/mol PS; (ii) refractive indices of binary mixed solvents as function of temperature and solvent composition, and dilute PS solutions at various polymer concentrations at 60 °C; (iii) refractive indices vs concentration of dilute PS solutions in 1-phenyldodecane at 23 and 60 °C, and Zimm plot of PS in 1-phenyldodecane at 23 °C; (iv) temperature dependence of the LS detector counts and the hydrodynamic radius of 0.5 vol % SEP 26−70 polymer in the 25/75 vol % 1-phenyldodecane/squalane mixed solvent upon heating and cooling; and (v) SAXS patterns of 1 vol % SEP 26−70 micelles in the 25/75 vol % phd/sql solvent at different temperatures 25−150 °C; and (v) unshifted $R(t)$ traces of 1 vol % SEP 26−70 and SEP 42−64 micelles in various binary mixed solvents at multiple temperatures (PDF)

■ AUTHOR INFORMATION

Corresponding Author

*E-mail: bates001@umn.edu, lodge@umn.edu.

ORCID

En Wang: 0000-0002-3271-7562

Dan Zhao: 0000-0001-8928-0691

Shuyi Xie: 0000-0001-7966-1239

Frank S. Bates: 0000-0003-3977-1278

Timothy P. Lodge: 0000-0001-5916-8834

Notes

The authors declare no competing financial interest.

■ ACKNOWLEDGMENTS

This work was supported by Infineum USA, L. P. and by the National Science Foundation Polymers Program through award DMR-1707578. The TR-SANS experiments were conducted at the High Flux Isotope Reactor in Oak Ridge National Laboratory, which is sponsored by the Scientific User Facilities Division, Office of Basic Energy Sciences, U.S. Department of Energy. We acknowledge Dr. Lilin He for help with TR-SANS experiments at ORNL. The SAXS experiments were conducted at DuPont-Northwestern-Dow Collaborative Access Team (DND-CAT) 5-ID at the Advanced Photon Source, Argonne National Laboratory, a U.S. Department of Energy (DOE) Office of Science User Facility operated for the DOE Office of Science by Argonne National Laboratory under Contract DE-AC02-06CH11357. Helpful discussions with Michael Rubinstein and David Morse are appreciated.

■ REFERENCES

(1) Lazzari, M.; López-Quintela, M. A. Block Copolymers as a Tool for Nanomaterial Fabrication. *Adv. Mater.* **2003**, *15*, 1583−1594.

(2) Glass, R.; Möller, M.; Spatz, J. P. Block Copolymer Micelle Nanolithography. *Nanotechnology* **2003**, *14*, 1153−1160.

(3) Hamley, I. W. Nanostructure Fabrication using Block Copolymers. *Nanotechnology* **2003**, *14*, 39−54.

(4) Jeong, B.; Bae, Y. H.; Lee, D. S.; Kim, S. W. Biodegradable Block Copolymers as Injectable Drug-Delivery Systems. *Nature* **1997**, *388*, 860−862.

(5) Li, Z.; Johnson, L. M.; Ricarte, R. G.; Yao, L. J.; Hillmyer, M. A.; Bates, F. S.; Lodge, T. P. Enhanced Performance of Blended Polymer Excipients in Delivering a Hydrophobic Drug through the Synergistic Action of Micelles and HPMCAS. *Langmuir* **2017**, *33*, 2837−2848.

(6) Li, Z.; Lenk, T. I.; Yao, L. J.; Bates, F. S.; Lodge, T. P. Maintaining Hydrophobic Drug Supersaturation in a Micelle Corona Reservoir. *Macromolecules* **2018**, *51*, 540−551.

(7) Anderson, W. Block Copolymers as Viscosity Index Improvers for Lubricating Oils. US3763044A, 1973.

(8) de Gennes, P. G. Conformations of Polymers Attached to an Interface. *Macromolecules* **1980**, *13*, 1069−1075.

(9) Halperin, A.; Tirrell, M.; Lodge, T. P. Tethered Chains in Polymer Microstuctures. *Adv. Polym. Sci.* **1992**, *100/1*, 31−71.

(10) Daoud, M.; Cotton, J. P. Star Shaped Polymers: A Model for the Conformation and its Concentration Dependence. *J. Phys. France* **1982**, *43*, 531−538.

(11) Halperin, A. Polymeric Micelles: A Star Model. *Macromolecules* **1987**, *20*, 2943−2946.

(12) Quintana, J. R.; Villacampa, M.; Muñoz, M.; Andrio, A.; Katime, I. A. Micellization of a Polystyrene-*block*-poly(ethylene/propylene) Copolymer in *n*-Alkanes. 1. Thermodynamic Study. *Macromolecules* **1992**, *25*, 3125−3128.

(13) Quintana, J. R.; Villacampa, M.; Andrio, A.; Muñoz, M.; Katime, I. A. Micellization of a Polystyrene-*block*-poly(ethylene/propylene) Copolymer in *n*-Alkanes. 2. Structural Study. *Macromolecules* **1992**, *25*, 3129−3136.

(14) Quintana, J. R.; Villacampa, M.; Katime, I. A. Micellization of a Polystyrene-*b*-poly(ethylene/propylene) Block Copolymer in *n*-Dodecane/1.4-Dioxane Mixtures. 1. Thermodynamics of Micellization. *Macromolecules* **1993**, *26*, 601−605.

(15) Quintana, J. R.; Villacampa, M.; Katime, I. A. Micellization of a Polystyrene-*b*-poly(ethylene/propylene) Block Copolymer in *n*-Dodecane/1.4-Dioxane Mixtures. 2. Structure and Dimensions of Micelles. *Macromolecules* **1993**, *26*, 606−611.

(16) Quintana, J. R.; Jáñez, M. D.; Villacampa, M.; Katime, I. Diblock Copolymer Micelles in Solvent Binary Mixtures. 1. Selective Solvent/Precipitant. *Macromolecules* **1995**, *28*, 4139−4143.

(17) Villacampa, M.; de Apodaca, E. D.; Quintana, J. R.; Katime, I. Diblock Copolymer Micelles in Solvent Binary Mixtures. 2. Selective Solvent/Good Solvent. *Macromolecules* **1995**, *28*, 4144−4149.

(18) Bang, J.; Viswanathan, K.; Lodge, T. P.; Park, M. J.; Char, K. Temperature-Dependent Micellar Structures in Poly(styrene-*b*-isoprene) Diblock Copolymer Solutions near the Critical Micelle Temperature. *J. Chem. Phys.* **2004**, *121*, 11489−11500.

(19) Bang, J.; Jain, S.; Li, Z.; Lodge, T. P.; Pedersen, J. S.; Kesselman, E.; Talmon, Y. Sphere, Cylinder, and Vesicle Nanoaggregates in Poly(styrene-*b*-isoprene) Diblock Copolymer Solutions. *Marcomolecules* **2006**, *39*, 1199−1208.

(20) Choi, S.; Bates, F. S.; Lodge, T. P. Structure of Poly(styrene-*b*-ethylene-*alt*-propylene) Diblock Copolymer Micelles in Squalane. *J. Phys. Chem. B* **2009**, *113*, 13840−13848.

(21) Choi, S.; Lee, W. B.; Lodge, T. P.; Bates, F. S. Structure of Poly(styrene-*b*-ethylene-*alt*-propylene) Diblock Copolymer Micelles in Binary Solvent Mixtures. *J. Polym. Sci., Part B: Polym. Phys.* **2016**, *54*, 22−31.

(22) Dormidontova, E. E. Micellization Kinetics in Block Copolymer Solutions: Scaling Model. *Macromolecules* **1999**, *32*, 7630−7644.

DOI: 10.1021/acs.macromol.9b01877
Macromolecules XXXX, XXX, XXX−XXX

(23) Haliloğlu, T.; Bahar, I.; Erman, B.; Mattice, W. L. Mechanisms of the Exchange of Diblock Copolymers between Micelles at Dynamic Equilibrium. *Macromolecules* **1996**, *29*, 4764−4771.
(24) Rharbi, Y. Fusion and Fragmentation Dynamics at Equilibrium in Triblock Copolymer Micelles. *Macromolecules* **2012**, *45*, 9823−9826.
(25) Halperin, A.; Alexander, S. Polymeric Micelles: Their Relaxation Kinetics. *Macromolecules* **1989**, *22*, 2403−2412.
(26) Halperin, A. On Micellar Exchange: The Role of the Insertion Penalty. *Macromolecules* **2011**, *44*, 5072−5074.
(27) Lund, R.; Willner, L.; Stellbrink, J.; Radulescu, A.; Richter, D. Tuning of Structure and Kinetics of Chain Exchange in Star-Like PEP-PEO Block Copolymer Micelles. *Phys. B* **2004**, *350*, E909−E912.
(28) Lund, R.; Willner, L.; Richter, D.; Dormidontova, E. E. Equilibrium Chain Exchange Kinetics of Diblock Copolymer Micelles: Tuning and Logarithmic Relaxation. *Macromolecules* **2006**, *39*, 4566−4575.
(29) Lund, R.; Willner, L.; Stellbrink, J.; Lindner, P.; Richter, D. Logarithmic Chain-Exchange Kinetics of Diblock Copolymer Micelles. *Phys. Rev. Lett.* **2006**, *96*, No. 068302.
(30) Choi, S.; Lodge, T. P.; Bates, F. S. Mechanism of Molecular Exchange in Diblock Copolymer Micelles: Hypersensitivity to Core Chain Length. *Phys. Rev. Lett.* **2010**, *104*, No. 047802.
(31) Li, Z.; Dormidontova, E. E. Equilibrium Chain Exchange Kinetics in Block Copolymer Micelle Solutions by Dissipative Particle Dynamics Simulations. *Soft Matter* **2011**, *7*, 4179−4188.
(32) Ma, Y.; Lodge, T. P. Chain Exchange Kinetics in Diblock Copolymer Micelles in Ionic Liquids: The Role of χ. *Macromolecules* **2016**, *49*, 9542−9552.
(33) Pedersen, J. S.; Gerstenberg, M. C. Scattering Form Factor of Block Copolymer Micelles. *Macromolecules* **1996**, *29*, 1363−1365.
(34) Pedersen, J. S.; Hamley, I. W.; Ryu, C. Y.; Lodge, T. P. Contrast Variation Small-Angle Neutron Scattering Study of the Structure of Block Copolymer Micelles in a Slightly Selective Solvent at Semidilute Concentrations. *Macromolecules* **2000**, *33*, 542−550.
(35) Pedersen, J. S. Structure Factors Effects in Small-Angle Scattering from Block Copolymer Micelles and Star Polymers. *J. Chem. Phys.* **2001**, *114*, 2839−2846.
(36) Pedersen, J. S.; Svaneborg, C. Scattering from Block Copolymer Micelles. *Curr. Opin. Colloid Interface Sci.* **2002**, *7*, 158−166.
(37) Pedersen, J. S.; Svaneborg, C.; Almdal, K.; Hamley, I. W.; Young, R. N. A Small-Angle Neutron and X-ray Contrast Variation Scattering Study of the Structure of Block Copolymer Micelles: Corona Shape and Excluded Volume Interactions. *Macromolecules* **2003**, *36*, 416−433.
(38) Lu, J.; Choi, S.; Bates, F. S.; Lodge, T. P. Molecular Exchange in Diblock Copolymer Micelles: Bimodal Distribution in Core-Block Molecular Weights. *ACS Macro Lett.* **2012**, *1*, 982−985.
(39) Lu, J.; Bates, F. S.; Lodge, T. P. Remarkable Effect of Molecular Architecture on Chain Exchange in Triblock Copolymer Micelles. *Macromolecules* **2015**, *48*, 2667−2676.
(40) Lu, J.; Bates, F. S.; Lodge, T. P. Addition of Corona Block Homopolymer Retards Chain Exchange in Solutions of Block Copolymer Micelles. *Macromolecules* **2016**, *49*, 1405−1413.
(41) Lai, C.; Russel, W. B.; Register, R. A. Phase Behavior of Styrene-Isoprene Diblock Copolymers in Strongly Selective Solvents. *Macromolecules* **2002**, *35*, 841−849.
(42) Hiemenz, P. C.; Lodge, T. P. *Polymer Chemistry*, 2nd ed.; CRC Press: Boca Raton, FL, 2007; pp 492−495.
(43) Richert, R.; Duvvuri, K.; Duong, L.-T. Dynamics of Glass-Forming Liquids. VII. Dielectric Relaxation of Supercooled *tris*-Naphthylbenzene, Squalane, and Decahydroisoquinoline. *J. Chem. Phys.* **2003**, *118*, 1828−1836.
(44) Hecksher, T.; Olsen, N. B.; Dyre, J. C. Model for the Alpha and Beta Shear Mechanical Properties of Supercooled Liquids and its Comparison to Squalane Data. *J. Chem. Phys.* **2017**, *146*, No. 154504.
(45) Milhet, M.; Pauly, J.; Coutinho, J. A. P.; Daridon, J.-L. Solid−Liquid Equilibria under High Pressure of Nine Pure *n*-Alkylbenzenes. *J. Chem. Eng. Data* **2008**, *53*, 233−237.
(46) Fox, T. G.; Flory, P. J. The Glass Temperature and Related Properties of Polystyrene. Influence of Molecular Weight. *J. Polym. Sci.* **1954**, *14*, 315−319.
(47) Wang, E.; Lu, J.; Bates, F. S.; Lodge, T. P. Effect of Corona Block Length on the Structure and Chain Exchange Kinetics of Block Copolymer Micelles. *Macromolecules* **2018**, *51*, 3563−3571.
(48) Williams, M. L.; Landel, R. F.; Ferry, J. D. The Temperature Dependence of Relaxation Mechanisms in Amorphous Polymers and Other Glass-forming Liquids. *J. Am. Chem. Soc.* **1955**, *77*, 3701−3707.
(49) Chapman, B. R.; Hamersky, M. W.; Milhaupt, J. M.; Kostelecky, C.; Lodge, T. P.; et al. Structure and Dynamics of Disordered Tetrablock Copolymers: Composition and Temperature Dependence of Local Friction. *Macromolecules* **1998**, *31*, 4562−4573.
(50) Bates, F. S.; Fredrickson, G. H. Block Copolymers − Designer Soft Materials. *Phys. Today* **1999**, *52*, 32−38.
(51) Radulescu, A.; Mathers, R. T.; Coates, G. W.; Richter, D.; Fetters, L. J. A SANS Study of the Self-Assembly in Solution of Syndiotactic Polypropylene Homopolymers, Syndiotactic Polypropylene-*block*-poly(ethylene-*co*-propylene) Diblock Copolymers, and an Alternating Atactic-Isotactic Multisegment Polypropylene. *Macromolecules* **2004**, *37*, 6962−6971.
(52) Fetters, L. J.; Lohse, D. J.; Richter, D.; Witten, T. A.; Zirkel, A. Connection between Polymer Molecular Weight, Density, Chain Dimensions, and Melt Viscoelastic Properties. *Macromolecules* **1994**, *27*, 4639−4647.
(53) Hoarfrost, M. L.; He, Y.; Lodge, T. P. Lower Critical Solution Temperature Phase Behavior of Poly(n-butyl methacrylate) in Ionic Liquid Mixtures. *Macromolecules* **2013**, *46*, 9464−9472.
(54) Lund, R.; Willner, L.; Lindner, P.; Richter, D. Structural Properties of Weakly Segregated PS-PB Block Copolymer Micelles in *n*-Alkanes: Solvent Entropy Effects. *Macromolecules* **2009**, *42*, 2686−2695.
(55) Lee, W.; Lee, H.; Cha, J.; Chang, T.; Hanley, K. J.; Lodge, T. P. Molecular Weight Distribution of Polystyrene Made by Anionic Polymerization. *Macromolecules* **2000**, *33*, 5111−5115.

DOI: 10.1021/acs.macromol.9b01877
Macromolecules XXXX, XXX, XXX−XXX